Journal of
Nanoscience and Nanotechnology
Vol. 12, 2387-2393, 2012

Preparation and Characterization of Electrospun Core Sheath Nanofibers from Multi-Walled Carbon Nanotubes and Poly(vinyl pyrrolidone)

Jianjun Miao[1, 2, 5, 6], Minoru Miyauchi[5, 6], Jonathan S. Dordick[1, 3, 4, 5, 6], and Robert J. Linhardt[1, 2, 3, 4, 5, 6, *]

[1] Departments of Chemical and Biological Engineering, [2] Chemistry and Chemical Biology, [3] Biology, [4] Biomedical Engineering, [5] Rensselaer Nanotechnology Center, and [6] Center for Biotechnology and Interdisciplinary Studies, Rensselaer Polytechnic Institute, 110 Eighth Street, Troy, NY, 12180, USA

Electrospinning is a versatile technique to prepare polymer fibers in nano to micrometer size ranges using very high electrostatic fields. Electrospun nanofibers with tunable porosity and high specific surface area have various applications, including chromatographic supports for protein separation, biomedical devices, tissue engineering and drug delivery matrices, and as key components in solar cells and supercapacitors. Unspinnable materials such as nanoparticles, nanorods, nanotubes or rigid conducting polymers can also be electrospun into fibers through co-axial electrospinning. In this study, we have prepared core-sheath nanofibers utilizing co-axial electrospinning. The core portion of these electrospun fibers consists of multi-walled carbon nanotubes and the sheath portion is poly(vinyl pyrrolidone) (PVP). Various morphologies were obtained by changing both core and sheath solution concentrations. The core-sheath nanofibers were characterized by scanning electron microscopy and transmission electron microscopy, to confirm core-sheath morphology, thermogravimetric analysis, and mechanical strength testing. The electrical conductivity of the surfaces of poly(vinyl pyrrolidone) fibers and poly(vinyl pyrrolidone)-multi-walled nanotube fibers were both 10^{-15} S/m. The highest bulk conductivity observed for the poly(vinyl pyrrolidone)-multi-walled nanotube fibers was 1.2×10^{-3} S/m.

Keywords: Electrospinning, Core-Sheath Fiber, Multi-Walled Carbon Nanotubes, Electrical Conductivity.

RESEARCH ARTICLE

1. INTRODUCTION

Electrospinning is a versatile technique used to produce nano- and microfibers under a high electrostatic field. The first prototype of electrospinning appeared in 1934 as a novel process for generating small diameter fibers.[1, 2] As new processes were developed, an increasing number of materials were electrospun into fibers with various applications ranging from fibers for protein purification and tissue engineering to fibers used for energy storage.[3] Generally only those materials with sufficient chain entanglement can be electrospun into fibers.[4] However, introducing co-axial electrospinning allows the use of nonspinnable materials, such as nanoparticles, carbon nanotubes or conjugated polymers, into fibers where they were fed into the fiber core through an inner needle and a spinnable supporting polymer solution was fed into the fiber sheath through an outer needle. For instance, a nonspinnable conductive polymer, poly[2-methoxy-5-(2-ethylhexyloxy)-1,4-phenylenevinylene] (MEH-PPV) in chloroform could be fed into an inner needle and a spinnable polymer, poly(vinyl pyrrolidone) (PVP) in ethanol/water could be fed into an outer needle at various feed ratios, to afford core-sheath nanofibers of MEHPPV-PVP.[5]

Among the nanoscale additives for improving physical performance of polymer composites, carbon nanotubes have drawn considerable attention since they were discovered by Iijima in 1991,[6] due to their unique properties for mechanical, electrical, and thermal resistance reinforcement when microscopically blended with polymer matrix.[7, 8] Well-dispersed multi-walled carbon nanotubes (MWNTs) in a polymer matrix were required to achieve these improvements. Low molecular weight surfactants or host polymers wrapped around the hydrophobic surface of MWNTs has been used for their dispersion in

*Author to whom correspondence should be addressed.

aqueous solution.[9, 10] Surface functionalization of MWNTs has also been used to increase the dispersibility in aqueous or organic solutions facilitating final composites formation.[11–13]

A number of electrospun polymer-MWNT composite nanofibers have been reported, including polyethylene oxide (PEO), poly(methylmethacrylate) (PMMA), poly(acrylonitrile) (PAN), and poly(ethylene terephthalate).[14] MWNTs dispersed in aqueous solutions of sodium dodecyl sulfate (SDS) or gum arabic have been used to prepare PEO/MWNTs.[15, 16] PMMA-MWNT dispersions have also been prepared from polymerization of MMA-oxidized MWNT dispersions.[17] Acid oxidized MWNTs, well dispersed in PAN/dimethylformamide (DMF) solution have been electrospun to form composite fibers showing a three-fold increased in tensile strength as a result of MWNT alignment within PAN fiber.[11] Few studies have investigated core-sheath MWNTs-polymer nanofibers. Ojha et al. reported a core sheath fiber made from PEO as core and PEO/MWNTs as sheath, in which MWNTs were dispersed in 3% gum arabic in water along with 4% PEO as sheath solution. The resulting bicomponent fiber has a much larger modulus than single component fiber at same effective MWNTs loading (0.25%). The enrichment/aggregation of MWNTs near the fiber surface accounts for the increased fiber stiffness.[18] Miyauchi et al. have first reported a core-sheath system based on natural polymer-cellulose as the sheath and MWNTs as the core. A 1.5% cellulose solution was prepared in 1-methyl-3-methylimidazolium acetate ([EMIM][OAc]) and MWNTs were dispersed in [EMIM][OAc] to form a MWNT gel. The surface conductivity of a resulting fiber mat was close to zero; however, after enzymatic removal of the surface cellulose using cellulase, the fiber conductivity reached as high as 10.7 S/m at 45% MWNT fiber loading.[19]

In the current study, nanocables or nanowires have been designed containing a core sheath nanofiber using MWNTs and PVP. MWNT concentration was varied in the core and PVP1300K concentration was varied in the sheath. The resulting core-sheath structures were characterized by transmission electron microscopy (TEM) and scanning electron microscopy (SEM), and thermal stability and tensile strength were also studied.

2. EXPERIMENTAL DETAILS

2.1. Materials and Methods

PVP of *Mw* 10,000 and 1,300,000 were obtained from Sigma-Aldrich and denoted as PVP10K and PVP1300K respectively. MWNTs were purchased from Cheap Tubes Inc., Vermont USA and used without further purification. The dimension of these carbon nanotubes was 20–30 nm in diameter and 10–30 μm in length, respectively, with 95% purity. All solvents were purchased from Fisher Scientific and used as received.

2.2. Preparation of Electrospinning Solutions

The sheath solutions, 9 and 12%, were made by dissolving PVP1300K in methanol. The core solutions, 1% and 2%, were made by dispersion of MWNTs in 0.5% and 1% PVP10K isopropanol solution, respectively, followed by ultrasonication. Concentrations of all solutions are indicated as wt%.

2.3. Electrospinning

Electrospinning was carried out on a spinneret instrument with a stainless steel outer needle and BD (Becton, Dickinson and company, Franklin Lakes, NJ) inner needle. Core-sheath fibers were obtained by a co-electrospinning process using a co-axial spinneret. For most runs the spinning parameters were as follows: the distance between spinneret and collector was 21 cm, and the electrostatic field was set at 0.5 kV/cm. The flow rate was controlled by a syringe pump and the core flow rate of the MWNT was 10 μL/min, and the sheath flow rate was 30 μL/min.

2.4. SEM Measurements

Field emission (FE)-SEM was performed to study the fiber surface and cross-sectional morphologies with a JEOL JSM-6335 FE-SEM (Tachikawa, Tokyo, Japan) equipped with a secondary electron detector at an accelerating voltage of 10 kV. The SEM samples were collected on aluminum foil, and cross-sectional samples were prepared by immersing the non-woven fiber mat in liquid nitrogen and then cut in half. Prior to the FE-SEM measurement, fiber mats were coated with a conductive film by sputtering gold in an argon atmosphere (0.3 mPa) using a sputter coater S-150 (Edwards Kniese & Co. GmbH, Marburg, Germany). Fiber diameter distribution was analyzed by image J software obtained from http://rsbweb.nih.gov/ij/.

2.5. TEM Measurements

TEM was performed on a Philips CM12 (Eindhoven, Amsterdam, Netherlands) at an accelerating voltage of 120 kV. Samples for TEM were obtained by depositing electrospun fibers onto 400 mesh copper grids under the spinneret for 2–3 s and dried in vacuum oven before TEM observation.

2.6. Mechanical Measurements

Tensile strength measurements were performed on an Instron Materials Testing Machine (Model 5843, Norwood, Massachusetts, USA) equipped with a 10 N static load cell and hydraulic grips (Instron 2712-001). Specimens were tested at 0.25-mm/min tension speeds, with a 5 mm gauge length. Both load and grip-to-grip distance was measured. Tensile strength was calculated by dividing the maximum load by the initial cross-sectional area of the samples.

2.7. Conductivity Measurements

The electrical conductivity of PVP-MWNT fibers was tested by a similar method used in reference with some modifications.[19] The removal of sheath by either vapor etching or heating at high temperature oven was not successful; instead, two razor blades were used as electrodes by cutting half depth into fiber mats. The distance between two parallel razor blades was 1 cm and the thickness of fiber mat was around 80–100 μm, and the width of fiber mat was 0.5 cm. The calculation of electrical conductivity is identical to that reported in the literature.[19]

2.8. Characterization of Thermal Behavior

Thermogravimetric analysis (TGA) was performed on a TA Instruments TGA Q50 (New Castle, Delaware, USA). The temperature was ramped up to 600 °C at 20 °C/min purged with nitrogen.

3. RESULTS AND DISCUSSION

3.1. Electrospinning

The core solution was prepared by dispersing MWNTs in 0.5 and 1% (w/w) PVP (10 kDa) isopropanol solution, which was stable for up to 6 months without any precipitation. High molecular weight PVP (1300 kDa), at the same percentage as used for PVP10K, was incapable of fully dispersing MWNTs probably due to lower chain mobility. Similar phenomena were reported for the PEO-MWNT system, in which sheath solution was made with relatively low molecular weigh surfactant gum arabic instead using high molecular weight PEO to disperse MWNTs.[18] Solvent polarity also has an effect on the dispersion of MWNTs. Initially, PVP methanol solution was used to disperse MWNTs; however, an obvious black precipitate remained at the bottom of the vial even after extensive sonication. Isopropanol was then chosen due to its lower polarity and higher affinity to hydrophobic MWNT surfaces compared to methanol. Two concentrations of MWNTs solution were prepared as 1% and 2%. The sheath solution was prepared by dissolving PVP1300K in methanol to make 9% and 12%. Ethanol and isopropanol were also used to prepare PVP1300K solution; however, the viscosity of solutions at same concentrations as prepared in isopropanol is much higher and the resulting electrospun fiber is thick. The electrospinning conditions are listed in Table I.

3.2. Morphological Characterization

The MWNTs used were purchased from Cheaptubes.com with a diameter specified in the product information sheet is 20–30 nm. The size distribution, measured by SEM, ranged from 15 nm to 50 nm, with a mean of 20–35 nm consistent with the suppliers product information sheet.

The electrospun fiber was collected on aluminum foil over 2–3 h and the resulting fiber mat was dried in vacuum oven overnight at room temperature. The fiber mat appeared black to off-white with gradually decreasing content of carbon nanotubes in fiber mat, PVP-MWNTs 9-2 to 12-1, Figure 2. As expected, fiber mats with PVP-MWNTs 9-2 showed the darkest color due to its high carbon nanotube loading (8.5 wt%). The color was homogeneously distributed throughout the PVP-MWNTs fiber mats, indicating an even distribution of MWNTs at the macroscopic level.

Improved thermal stability of the PVP-MWNTs core sheath fiber was expected compared to PVP fibers due to high stability of MWNTs. As shown in Figure 3, the thermal decomposition behavior of core-sheath PVP-MWNTs fiber was enhanced compared to single component PVP fiber. The decomposition peaks in all four core-sheath fibers shifted to higher temperatures (15–16 °C), indicating enhanced thermal stability resulting from the incorporation of MWNTs (Fig. 3(b)). The residual weight percent also increased as expected with increasing amount of carbon nanotube content within the PVP fiber mat (Fig. 3(a)).

The fiber morphology and size distribution for different electrospinning conditions are shown in Figure 4. A small amount of beads on string morphology was observed for PVP-MWNTs 9-1; however, the quality of the fibers could be improved by increasing the carbon nanotube amount and sheath solution concentration. Fiber thickness decreased slightly as the content of MWNTs in the fiber for sample pairs increased, PVP-MWNTs 9-1/9-2 and 12-1/12-2 (Table II). Increasing the sheath solution concentration also increased the final fiber thickness by approximately two-fold.

The nanofibers were examined by TEM to investigate and verify the core sheath morphology of electrospun PVP-MWNTs. The TEM images (Fig. 5) show a sharp

Table I. Electrospinning conditions for four experiments.

Sample (PVP-MWNTs)	PVP1300k Conc. (%)	MWNTs Conc. (%)	PVP10k Conc. (%)	PVP FR (μL/min)	MWNTs FR (μL/min)	Voltage (kV)	Distance (cm)
9-2	9.0	1.0	0.25	30	10	10	21
9-2	9.0	2.0	0.50	30	10	10	21
12-1	12.0	1.0	0.25	30	10	10	21
12-2	12.0	2.0	0.50	30	10	12	21

Conc.: concentration.

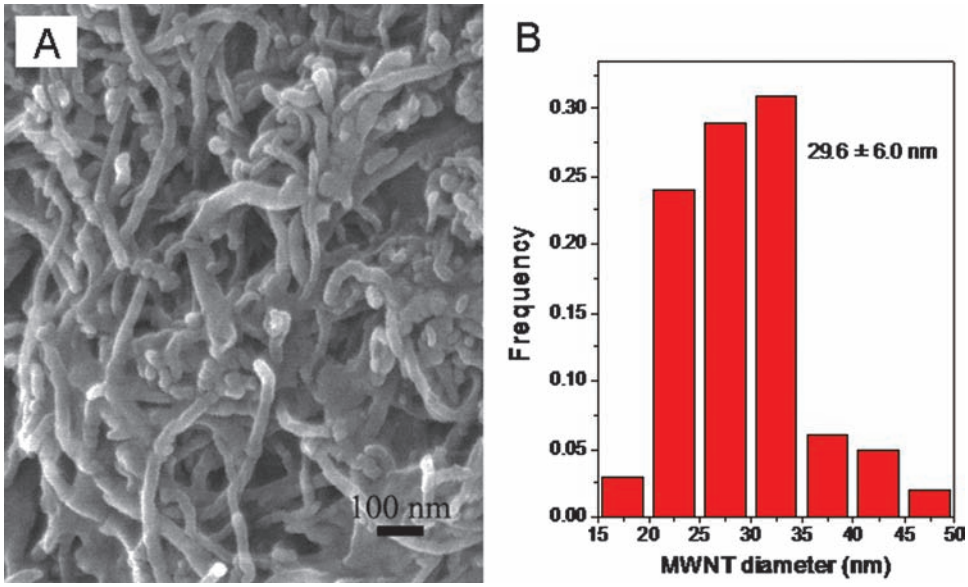

Fig. 1. SEM image (A) and size distribution (B) of as received MWNTs. The average size of as received MWNTs is 29.6 nm with 6 nm as standard deviation.

RESEARCH ARTICLE

contrast between center and edge of fiber in all four samples. These images clearly demonstrate core-sheath morphology for the carbon nanotube core and PVP sheath due to the high electron density difference between these materials. The clear boundary also indicates no obvious diffusion of carbon nanotubes into the sheath, and a core composed primarily of MWNTs. Due to the thick nature of the fibers, individual carbon nanotubes could not be observed by TEM. Thus, further investigation was conducted using FE-SEM. The FE-SEM images of fiber cross-section (Fig. 6), show individual carbon nanotubes protruding out of the fiber fractured surface and the amount of protruding carbon nanotubes increased with loading concentration, suggesting excellent dispersion of MWNTs by PVP and a homogenous orientation of carbon nanotubes along the fiber axis. FE-SEM also showed surface morphologies for individual fibers. With low loadings

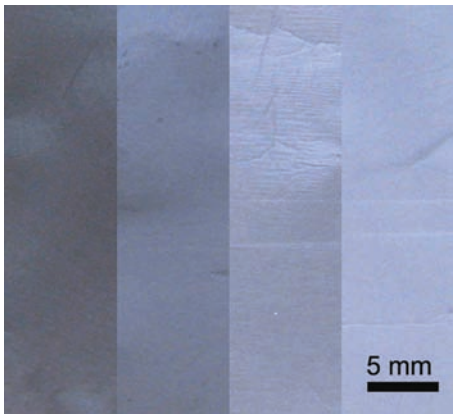

Fig. 2. Electrospun fiber mats from left to right, PVP-MWNTs 9-2, 12-2, 9-1 and 12-1.

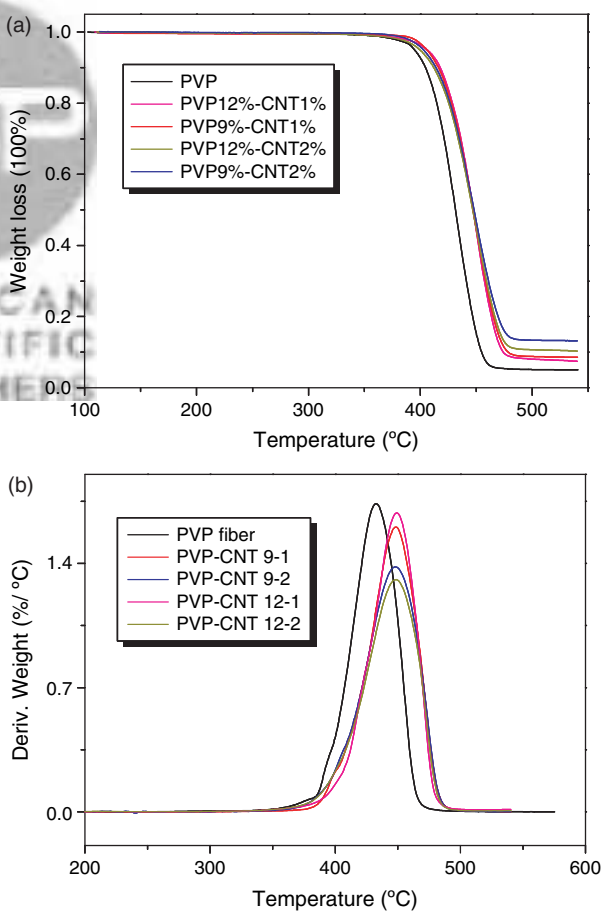

Fig. 3. Thermalgravetric analysis (TGA) of PVP-MWNTs core sheath fiber mats.

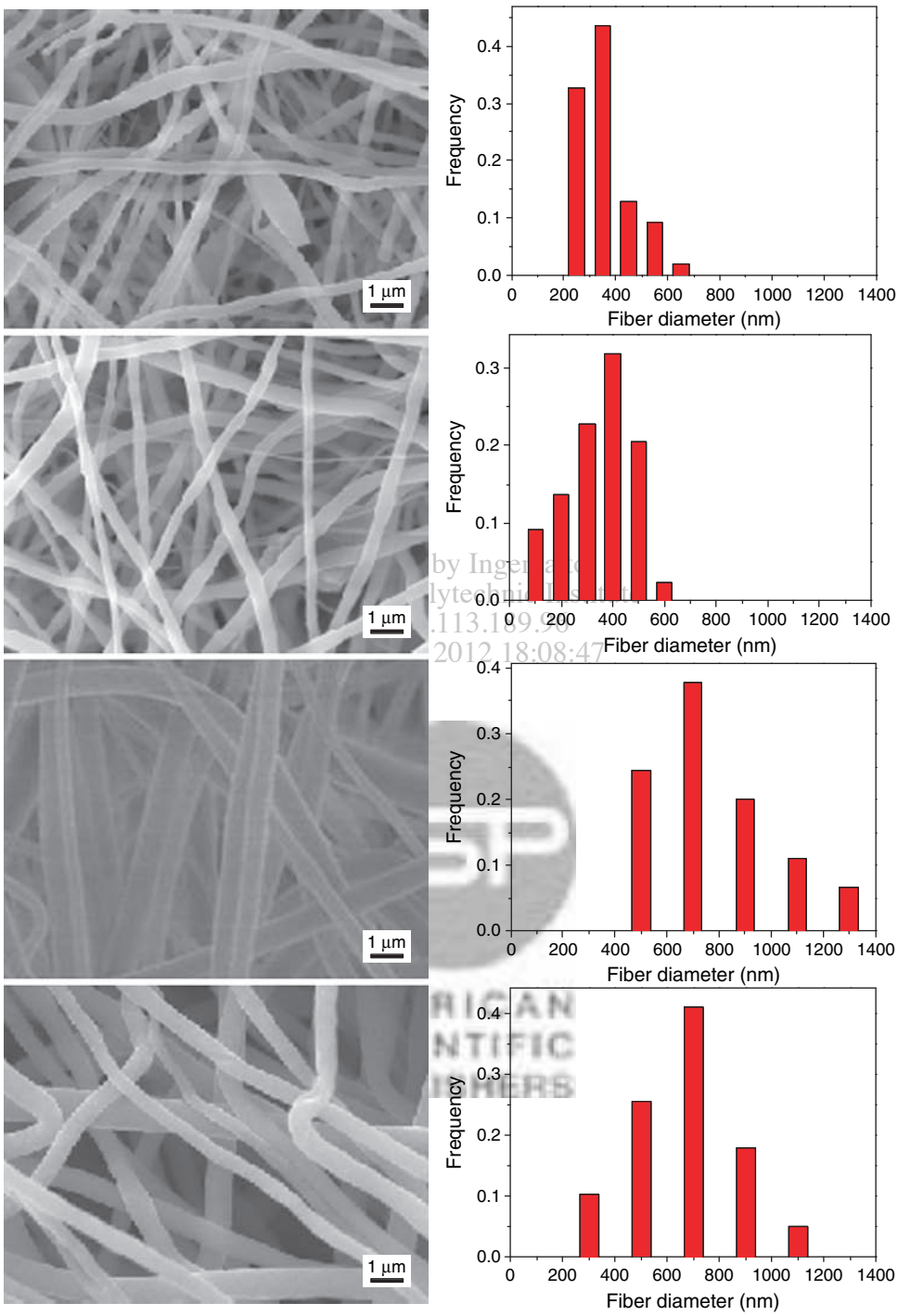

Fig. 4. SEM images and size distribution of PVP-MWNTs 9-1, 9-2, 12-1 and 12-2 from top to bottom.

of carbon nanotubes, the fiber surface was smooth; however, the fiber surface became slightly rough when loading of carbon nanotubes was doubled.

To further investigate the core-sheath structure of MWNT-PVP fiber mats, chemical etching of nanofibers was performed to remove PVP and leave the MWNTs intact.[20] The electrospun fibers were collected on silicon wafer, and then the fiber was subjected overnight to saturated isopropanol vapor at room temperature in a sealed vial. PVP easily absorbed isopropanol vapor and when adequate isopropanol was absorbed, PVP dissolved into condensed isopropanol solution and spread over the silicon wafer. The carbon nanotubes should remain together even though the PVP was dissolved only if they formed tight bundles within the fiber during electrospinning. Core-sheath MWNT-PVP fibers, saturated by

Table II. Summary of average fiber thickness of PVP-MWNTs 9-1, 9-2, 12-1 and 12-2.

Sample (PVP-CNT)	Average size (nm)
9-1	355 + / − 95
9-2	348 + / − 125
12-1	779 + / − 236
12-2	652 + / − 192

isopropanol, were then dried in a vacuum oven for 2 h to remove any residual solvent before subjecting to FE-SEM. The MWNT-PVP 9-1 fibers on silicon wafer before vapor treatment are as thin as 300 nm (Fig. 7(A)). After vapor treatment a carbon nanotube bundle was observed (Fig. 7(B)) with average diameter of 70 nm composing of about 4-5 paralled carbon nanotubes and with length up to 1 μm. We hypothesize that the MWNT bundle is formed during electrospinning by a confinement effect resulting from the PVP sheath.

3.3. Mechanical Testing

Tensile stress testing was performed to determine any changes in mechanical properties due to the core-sheath nature of the fibers. The typical stress-strain relationship can be determined from their corresponding curves. The tensile strength (Table III) was determined for five samples including control neat PVP fiber mat (electrospun from 9 wt% methanol solution). The specimen tested for mechanical strength had the dimensions of 15 mm long, 5 mm wide, with a thickness of 60–80 μm as measured using a micrometer. The gauge width was 5 mm. The strain rate is 0.25 mm/min. The tensile strength was calculated with maximum loading divided by cross-sectional area. The neat PVP fiber mat had highest tensile strength among the five samples tested (Table III) and increasing the amount of carbon nanotubes in the fiber caused a decreased tensile strength. The change of Young's modulus, resulting from an increased loading of MWNTs, was different from that of tensile strength. At low MWNT loadings, for PVP-MWNTs 9-1 and PVP-MWNTs 12-1, the modulus almost doubled compared to the neat PVP fiber. At high MWNT loadings, PVP-MWNTs 9-2 and PVP-MWNTs 12-2, the modulus decreased significantly to a value similar to neat PVP fiber mat. The enhancement of tensile modulus, compared to tensile strength at lower carbon nanotube loading, indicates that the reinforcement effect of carbon nanotubes is more prominent in the initial stress region than in the close-to-yield region. This can be explained by the carbon nanotubes, well dispersed

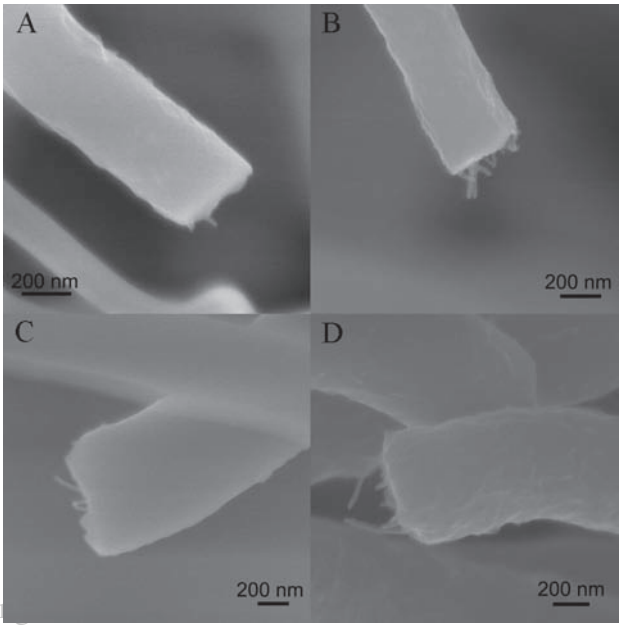

Fig. 6. SEM images of fiber cross-section from (A)-(D) PVP-MWNTs 9-1, 9-2, 12-1, and 12-2.

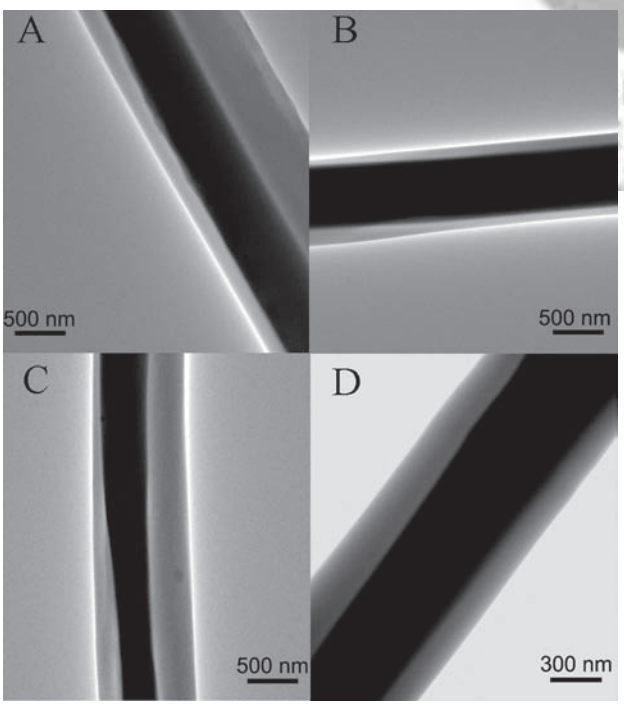

Fig. 5. Bright fields of TEM images, from (A) to (D) PVP-MWNTs 9-1, 9-2, 12-1 and 12-2.

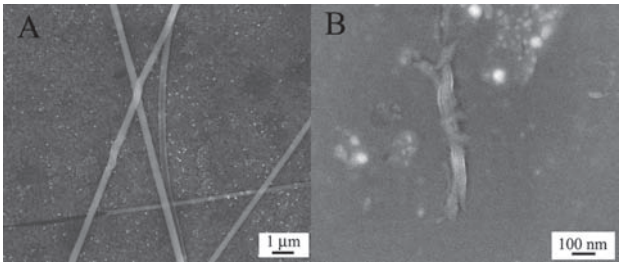

Fig. 7. SEM images of fiber etching with isopropanol vapor, (A) before and (B) after etching with isopropanol vapor at room temperature.

RESEARCH ARTICLE

Table III. Mechanical properties of MWNTs-PVP fiber mat.

PVP/MWNTS wt% in solution (wt% in fiber)	Tensile strength (MPa)	Tensile strain (%)	Youngs modulus (MPa)
9/1 (95.3/3.8)	2.30 ± 0.08	19.0 ± 2.0	90.8 ± 3.2
9/2 (89.8/8.5)	1.08 ± 0.29	19.0 ± 2.4	41.8 ± 1.6
12/1 (95.6/3)	2.77 ± 0.02	34.0 ± 1.4	95.1 ± 3.9
12/2 (92.0/5.7)	1.11 ± 0.13	32.0 ± 1.4	57.6 ± 2.3
Neat PVP fiber	2.86 ± 0.25	22.0 ± 2.8	54.3 ± 2.8

in PVP10K, helping to extend the van der Waals interaction from interface between PVP1300K matrix sheath and carbon nanotubes core to whole core region. Thus, in the initial strain region, the load transfer from sheath to core was most efficient. Similar phenomena were reported for PEO/MWNTS core-sheath fiber mats, in which the modulus at 0.25% effective carbon nanotube concentration was much larger than that of neat PEO fiber despite having a reduced tensile strength.[18] Further increasing the amount of carbon nanotubes, PVP-MWNTs 9-2 and PVP-MWNTs 12-2, caused carbon nanotube agglomeration within the core and reduced load transfer from sheath to core. This effect is presumably due to fewer interfaces between the carbon nanotube core and the PVP sheath matrix. A similar phenomenon was also reported in the fibers having a carbon nanotube core and a cellulose sheath.[19]

3.4. Conductivity Measurements

The surface of fiber mats for neat PVP and other four PVP-MWNT samples all showed low electrical conductivity of 10^{-15} S/m, and thus, could be considered as an insulation surface. We attempted to remove the sheath of fiber mat to test the bulk conductivity by either isopropanol vapor etching or high temperature calcinations, but these methods failed due to a loss of fiber mat integrity after PVP was removed. A nondestructive method, involving cutting into fiber mats with a razor blade and connecting the mat to electrodes, was next used. Low electrical conductivity was observed, with highest conducting mat showing 1.2×10^{-3} S/m for PVP-MWNT 9-2. This value is 4-orders of magnitude lower than that obtained with cellulose-MWNTs at 45% loading, as a result of the much lower MWNT loading (8.5%) in current core-sheath fiber mats.[19] Higher MWNT loading and more accurate measurement methods will be required to further improve and demonstrate high electrical conductivity in core sheath fibers.

4. CONCLUSIONS

Core-sheath nanofibers of MWNTs and PVP have been prepared using co-axial electrospinning. The core-sheath morphology has been confirmed by both TEM and SEM. A certain degree of alignment of carbon nanotube within fiber was found and chemical vapor etching verified the carbon nanotube bundle was formed during electrospinning, due to the confinement effect from PVP sheath. Mechanical testing indicated that a neat PVP fiber mat had the highest tensile strength with increased of carbon nanotube loading decreasing the tensile strength due to inefficient loading transfer from PVP sheath to carbon nanotube core. Electrical conductivity testing of the neat PVP fiber and PVP-MWNT fiber surface showed conductivity of 10^{-15} S/m. The highest bulk conductivity found on PVP-MWNT 9-2 was 1.2×10^{-3} S/m.

Acknowledgments: We gratefully acknowledge JNC Corporation, Tokyo, Japan, and the Rensselaer Nanotechnology Center for their support of our research on electrospinning.

References and Notes

1. A. Formhals, US Pat. NO. 1,975,504 1934.
2. A. Formhals, US Pat. NO. 2,169,962 1939.
3. V. Thavasi, G. Singh, and S. Ramakrishna, *Energy Environ. Sci.* 1, 205 **(2008)**.
4. M. G. McKee, J. M. Layman, M. P. Cashion, and T. E. Long, *Science* 311, 353 **(2006)**.
5. D. Li, A. Babel, S. A. Jenekhe, and Y. N. Xia, *Adv. Mater.* 16, 2062 **(2004)**.
6. S. Iijima, *Nature* 354, 56 **(1991)**.
7. R. Sen, B. Zhao, D. Perea, M. E. Itkis, H. Hu, J. Love, E. Bekyarova, and R. C. Haddon, *Nano Lett.* 4, 459 **(2004)**.
8. H. H. Ye, H. Lam, N. Titchenal, Y. Gogotsi, and F. Ko, *Appl. Phys. Lett.* 85, 1775 **(2004)**.
9. S. Mazinani, A. Ajji, and C. Dubois, *Polymer* 50, 3329 **(2009)**.
10. P. Lu and Y. L. Hsieh, *ACS Applied Materials & Interfaces* 2, 2413 **(2010)**.
11. J. J. Ge, H. Q. Hou, Q. Li, M. J. Graham, A. Greiner, D. H. Reneker, F. W. Harris, and S. Z. D. Cheng, *J. Am. Chem. Soc.* 126, 15754 **(2004)**.
12. J. S. Jeong, J. S. Moon, S. Y. Jeon, J. H. Park, P. S. Alegaonkar, and J. B. Yoo, *Thin Solid Films* 515, 5136 **(2007)**.
13. Y. Ji, C. Li, G. Wang, J. Koo, S. Ge, B. Li, J. Jiang, B. Herzberg, T. Klein, S. Chen, J. C. Sokolov, and M. H. Rafailovich, *Epl* 84, 56002 **(2008)**.
14. B. W. Ahn, Y. S. Chi, and T. J. Kang, *J. Appl. Polym. Sci.* 110, 4055 **(2008)**.
15. J. Y. Lim, C. K. Lee, S. J. Kim, I. Y. Kim, and S. I. Kim, *J. Macromol. Sci., Pure Appl. Chem.* 43, 785 **(2006)**.
16. S. D. McCullen, D. R. Stevens, W. A. Roberts, S. S. Ojha, L. I. Clarke, and R. E. Gorga, *Macromolecules* 40, 997 **(2007)**.
17. J. H. Sung, H. S. Kim, H. J. Jin, H. J. Choi, and I. J. Chin, *Macromolecules* 37, 9899 **(2004)**.
18. S. S. Ojha, D. R. Stevens, K. Stano, T. Hoffman, L. I. Clarke, and R. E. Gorga, *Macromolecules* 41, 2509 **(2008)**.
19. M. Miyauchi, J. J. Miao, T. J. Simmons, J. W. Lee, T. V. Doherty, J. S. Dordick, and R. J. Linhardt, *Biomacromolecules* 11, 2440 **(2010)**.
20. J. B. Gao, A. P. Yu, M. E. Itkis, E. Bekyarova, B. Zhao, S. Niyogi, and R. C. Haddon, *J. Am. Chem. Soc.* 126, 16698 **(2004)**.

Received: 30 May 2011. Accepted: 7 September 2011.

RESEARCH ARTICLE